FEMS Yeast Research, 2023, 21, 1–8
DOI: 10.1093/femsyr/foad053
Research Article

Heterologous pulcherrimin production in *Saccharomyces cerevisiae* confers inhibitory activity on *Botrytis* conidiation

Florian M. Freimoser[1,*], Marina Mahler[1], Mark McCullough[2], Alexander O. Brachmann[3], Lukas Nägeli[1], Maja Hilber-Bodmer[1], Jörn Piel[3], Stefan Hoffmann[2], Yizhi Cai[2,*]

[1]Agroscope, Research Division Plant Protection, Route de Duillier 60, 1260 Nyon 1, Switzerland
[2]Manchester Institute of Biotechnology and School of Chemistry, University of Manchester, Manchester, UK
[3]Institute of Microbiology, Eidgenössische Technische Hochschule (ETH) Zürich, 8093 Zürich, Switzerland
*Corresponding authors. E-mail: florian.freimoser@agroscope.admin.ch; yizhi.cai@manchester.ac.uk
Editor: Miguel Teixeira

Abstract

Pulcherrimin is an iron (III) chelate of pulcherriminic acid that plays a role in antagonistic microbial interactions, iron metabolism, and stress responses. Some bacteria and yeasts produce pulcherriminic acid, but so far, pulcherrimin could not be produced in *Saccharomyces cerevisiae*. Here, multiple integrations of the *Metschnikowia pulcherrima PUL1* and *PUL2* genes in the *S. cerevisiae* genome resulted in red colonies, which indicated pulcherrimin formation. The coloration correlated positively and significantly with the number of *PUL1* and *PUL2* genes. The presence of pulcherriminic acid was confirmed by mass spectrometry. *In vitro* competition assays with the plant pathogenic fungus *Botrytis caroliana* revealed inhibitory activity on conidiation by an engineered, strong pulcherrimin-producing *S. cerevisiae* strain. We demonstrate that the *PUL1* and *PUL2* genes from *M. pulcherrima*, in multiple copies, are sufficient to transfer pulcherrimin production to *S. cerevisiae* and represent the starting point for engineering and optimizing this biosynthetic pathway in the future.

Keywords: biocontrol; *Metschnikowia*; pulcherrimin; siderophore; iron; antagonism; *Saccharomyces cerevisiae*; competition; conidiation; *Botrytis*

Introduction

The ascomycete yeast *Metschnikowia pulcherrima* is frequently isolated from environmental samples and reported to antagonize fungal plant pathogens, but knowledge of this activity at the molecular level is limited. In a comparative analysis of 40 different yeast species and isolates, *M. pulcherrima* (isolate APC 1.2) was the most antagonistic yeast against filamentous fungi (Hilber-Bodmer et al. 2017). This species has simple growth requirements, is highly stable during storage, can colonize plants, and has shown promising activity against apple postharvest diseases in field trials (Bühlmann et al. 2021). To improve biocontrol reliability and efficacy, it is mandatory to understand the mechanisms responsible for the strong antagonistic activity of *M. pulcherrima* at a fundamental level. Only with this knowledge will it be possible to select and optimize strains, production, formulation, and application of this promising biocontrol yeast species.

Pulcherrimin is a red pigment that forms spontaneously in the presence of iron by a non-enzymatic reaction (Melvydas et al. 2016). It is the most remarkable characteristic of *M. pulcherrima* and confers a dark red color to colonies growing on iron-containing media. The compound is an iron (III) chelate of pulcherriminic acid (2,5-diisobutyl-3,6-dihydroxy-pyrazine-1,4-dioxide), which is formed by the oxidation of cyclodileucine [cyclo(Leu–Leu)] (MacDonald 1965). Cyclodipeptides such as cyclo(Leu–Leu) belong to the diketopiperazine family of secondary metabolites, some of which have been implicated in antibiotic activities, radical scavenging, quorum sensing, or immunosuppression (Bonnefond et al. 2011, Borthwick 2012, Furukawa et al. 2012, Bellezza et al. 2014, Mishra et al. 2017).

Pulcherrimin was first described in yeasts >60 years ago (Canale-Parola 1963), but little is known about its functions and biosynthesis in eukaryotes. Only recently, a cluster of four genes (*PUL1-4*) involved in its biosynthesis and transport in fungi have been identified in the yeast *Kluyveromyces lactis* (Krause et al. 2018). The core pulcherriminic acid biosynthesis genes are *PUL1*, encoding a cyclodileucine synthetase, and the cytochrome P450 gene *PUL2* (Pul2 catalyzes the oxidation of cyclodileucine to pulcherriminic acid) (Krause et al. 2018). However, pulcherrimin has not been produced in *Saccharomyces cerevisiae* by heterologously expressing *PUL1* and *PUL2* or the bacterial pulcherrimin biosynthesis genes (see below) and the biochemical function of *PUL1* has not been confirmed (Krause et al. 2018). Interestingly, many yeasts have lost the genes encoding the pulcherrimin synthesizing enzymes Pul1 and Pul2, but still contain *PUL3* and *PUL4* genes, encoding a transporter and regulatory protein, respectively (Krause et al. 2018). Such yeasts are able to utilize pulcherrimin produced by other yeasts, but are unable to produce the siderophore themselves (*S. cerevisiae* is such a species) (Krause et al. 2018). Naturally occurring *M. pulcherrima* mutants (with a premature stop codon in the chromatin regulator gene *SNF2*) devoid of pulcherrimin exhib-

Received 8 August 2023; **accepted** 21 December 2023

ited reduced antagonistic activity (Gore-Lloyd et al. 2019). However, these strains still antagonize plant pathogenic fungi such as *Botrytis caroliniana*, albeit less efficiently than the wildtype. While iron chelation by pulcherriminic acid is thought to cause iron depletion and to mediate the antimicrobial activity (Sipiczki 2006, Saravanakumar et al. 2008, Wang et al. 2018), this activity has not been experimentally proven. Evidently, pulcherrimin is also not the only mode of action employed by *M. pulcherrima* and likely other pulcherrimin-producing, antagonistic yeasts and bacteria (Gore-Lloyd et al. 2019). Other factors that are independent of pulcherrimin, for example secreted enzymes or volatiles, are likely also involved in mediating antagonistic activity (Freimoser et al. 2019). The antimicrobial activity of pulcherrimin-producing organisms may also be conferred by pulcherrimin precursors or degradation products, be due to a regulatory effect on plant, fungal, or bacterial responses and therefore be independent of iron, or result from a defense reaction against toxic iron levels (Kluyver et al. 1953, Sipiczki 2006, Kántor et al. 2015). The biological function and metabolism of pulcherrimin is thus not well characterized in yeasts and in general poorly understood.

Besides yeasts, pulcherrimin is also produced by certain bacteria such as *Bacillus licheniformis*, where the two genes *yvmC* and *cypX*, encoding a cyclodipeptide synthase and cytochrome P450 oxidase, respectively, are responsible for its biosynthesis (Tang et al. 2006, Gondry et al. 2009, Cryle et al. 2010). Expression of *yvmC* and *cypX* and the formation of pulcherrimin are intricately regulated by a complex interplay of factors such as growth stage, iron availability, or environmental stress (Randazzo et al. 2016, Wang et al. 2018). Most recent studies suggest that iron precipitation by pulcherriminic acid production constitutes a yet unknown iron managing system in bacteria that confers protection against oxidative stress (Charron-Lamoureux et al. 2022, Angelini et al. 2023). In *B. licheniformis*, high pulcherrimin production was engineered by increasing the supply of leucine, limiting branched-chain fatty acid metabolism, overexpressing a leucine-tRNA synthase gene, promoter exchange of the yvmC–cypX synthetase cluster, and overexpression of a pulcherriminic acid exporter gene (Wang et al. 2020, Yuan et al. 2020). In contrast, it has so far not been possible to engineer pulcherrimin production by heterologously expressing the eukaryotic pulcherrimin synthesis genes *PUL1* and *PUL2* (Krause et al. 2018, Widodo and Billerbeck 2022).

In the work reported here, we integrated random copy numbers of the *M. pulcherrima PUL1* and *PUL2* in the *S. cerevisiae* genome, confirmed pulcherrimin production in the engineered strains, and demonstrated that pulcherrimin formation correlates positively with the *PUL1* and *PUL2* copy number. Furthermore, a *S. cerevisiae* strain producing high pulcherrimin levels inhibited conidiogenesis of the plant pathogenic fungus *Botrytis* more strongly than a control strain. This heterologous *S. cerevisiae*-model for pulcherrimin formation can be instrumental to elucidate biological functions of this metabolite, investigate pulcherrimin metabolism in yeasts, and engineer pulcherrimin and cyclodipeptide production.

Material and methods

Strains and culture conditions

For heterologous expression, the *S. cerevisiae* strains BY4741 (MATa *his3Δ1 leu2Δ0 met15Δ0 ura3Δ0*) was used. All yeast strains were routinely maintained on yeast extract peptone dextrose or potato dextrose agar (PDA, Formedium™, Norfolk, United Kingdom and Becton, Dickinson and Company, Le Pont de Claix, France, respectively). For the selection of transformants expressing *PUL1* and *PUL2*, yeast nitrogen base (YNB) medium with a complete amino acid supplement lacking leucine (-Leu) was used (Formedium™, Norfolk, United Kingdom). *Botrytis caroliniana* X.P. Li & G. Schnabel (isolate EC 1.05, SH0986633.09FU) was cultivated on PDA (Becton, Dickinson and Company, Le Pont de Claix, France). Plates were incubated at 22°C or 30°C and the cultures were transferred to fresh plates weekly.

Cloning of PUL genes

The *PUL1* (MPUL0C04990) and *PUL2* (MPUL0C04980) sequences were obtained from the *M. pulcherrima* APC 1.2 genome (Gore-Lloyd et al. 2019). For expression in *S. cerevisiae*, all CTG codons were changed to AGT (6 and 8 codons for *PUL1* and *PUL2*, respectively). The sequences were codon optimized for *S. cerevisiae* and synthesized at Twist Bioscience (Twist Bioscience, South San Francisco, CA, USA). The genes were cloned by using ~~the~~ Golden Gate Cloning and the yeast Modular Cloning (MoClo) PYTK toolkit (Lee et al. 2015). To make the two genes compatible with the PYTK standard for type 3 (ORF) parts, two codons for amino acid residues (a glycine and serine) were introduced before the STOP for *PUL1* and *PUL2*. Standard Golden Gate Cloning protocols and enzymes from New England Biolabs (obtained through BioConcept Ltd, Allschwil, Switzerland) were used. All newly generated level 0 parts (*PUL1* and *PUL2* genes) were verified by Sanger sequencing (at Microsynth AG, Balgach, Switzerland). Genes were cloned with the *TDH3* promoter (P_{TDH3}) and *TDH1* terminator (T_{TDH1}) and the *LEU2* gene was used as a marker. The genes were integrated as one transcriptional unit in the *URA3* locus and insertions were confirmed by PCR.

Oxford nanopore sequencing of strains

High-molecular genomic DNA extraction was performed with the Macherey Nagel NucleoBond HMW DNA kit. Yeast cultures were grown to late log phase (OD_{600} of about 1.5) and DNA was extracted from 100–150 OD_{600} unit equivalents according to the manufacturer's instructions with enzymatic lysis of yeast cell walls. Genomic DNA library preparation used ONT's ligation sequencing kit SQK-LSK109 with a unique barcode for each strain (kits EXP-NDB104 and EXP-NDB114). Barcoded gDNA concentration was determined using a Qubit dsDNA BR kit and equimolar amounts for each sample were combined into a library. The pooled gDNA library (~700 ng) was loaded onto a R9.4.1 chemistry FLO-MIN106D SpotON flow cell in a MinION Mk1B device. Nanopore sequencing was undertaken using ONTs' MinKNOW v22.03.5. Fast5 files were basecalled using ONTs' Guppy software v6.1.7 (GPU) and default parameters (qscore filtering and demultiplexing). Summary data relating to the size, length, and quality of reads for the sequencing run and particular strains were obtained using NanoComp v1.19.0 and NanoPlot v1.40.0 (De Coster et al. 2018) (Supplementary Table S1).

Alignment

Prior to alignment, reads with chimeric duplexes were detected and split using ONT's Duplex Tools v0.3.2 (Duplex Tools 2023) "split_on_adapter" function with parameters "–allow_multiple_splits," and "Native." Split reads for each sample then underwent filtering using Chopper v0.2.0 to remove resultant short (<500 bp) and/or low quality reads (Phred < 9) (De Coster et al. 2018, Coster 2023). Sample reads were aligned against *S. cerevisiae* strain BY4741 reference using Minimap2 v2.17 (parameters -ax map-ont index) (Li 2018, 2021). Sequence alignment/map

files were sorted, binarized, and indexed using Samtools v1.15.1 (Li et al. 2009). Structural variants were inferred for each strain using Sniffles v2.0.6 (parameter "–minsupport auto" and reference BY4741) to validate the integration sites (Sedlazeck et al. 2018).

De novo genome assembly and comparison of assemblies

Sequencing reads for each strain underwent *de novo* draft genome assembly to infer the chromosome integrated vector gene profiles and orientations by either using Flye v2.8.1 (–nano-raw –iterations 3—genome-size 12.5 m, repeat graph implementation, automatically detect chimers) or Canu v2.1.1 (–genomeSize = 12.5 m, correctedErrorRate = 0.15, stopOnLowCoverage = 5, minInputCoverage = 5; adaptive *k*-mer weighting) (Koren et al. 2017, Kolmogorov et al. 2019). Draft genome assemblies underwent homology-based correction, scaffolding, and renaming against the reference genome using RagTag v2.1.0 correct (-f 500 -T ont) and scaffold (-f 500 -u) (Alonge et al. 2022). The assemblies were inspected through the software Bandage v0.8.1 (Wick et al. 2015). BLAST searches were undertaken to assess integration profiles for vector sequences (parameters: 100 nt alignment length, 50% query coverage, 90% identity, *e*-value = $1e-10$). Where both assembly methods produced different integration profiles, the quality of draft assemblies were compared with QUAST v5.2.0 (parameters: fungus, circos, split-scaffolds, nanopore reads, and BY4741 reference and features) (Gurevich et al. 2013). Quast is a tool to evaluate genome assemblies, but also allows scrutiny of chromosomes of interest via Circos and the Icarus viewer. Assembly quality metric are provided in Supplementary Table S1.

Identification of cyclodileucine and pulcherriminic acid

The pulcherrimin precursors cyclodileucine and pulcherriminic acid were identified as previously described (Gore-Lloyd et al. 2019). In short, metabolites were collected on Amberlite XAD16N beads (Sigma–Aldrich Chemie GmbH, Buchs, Switzerland) and eluted with methanol. Samples were analyzed by ultra-performance liquid chromatography-high resolution heated electrospray ionization mass spectrometry (UPLC HR HESI-MS).

Competition assays

Binary competition assays were carried out similar to a previously published protocol (Hilber-Bodmer et al. 2017), but adjustments to account for the different growth preferences of *S. cerevisiae* and plant pathogenic fungi were made. Yeast cells (OD_{600} of 0.01) were collected in water and 15 μl were spread on one half of 5.5 cm diameter PDA plates. After preincubation at 22°C (14–20 days), *B. caroliniana* (conidial suspension, OD_{600} of 0.1, 5 μl) was added to the center of the plate and the assays were incubated at 22°C for 10–14 days. The production of *B. caroliniana* conidia was assessed by removing an agar plug (~5 mm in diameter), suspension in water, and measuring the optical density at 600 nm (OD_{600}; preliminary experiments had shown that hemocytometer counts of conidia correlated well with OD_{600} measurements). The average optical density of three replicates was calculated. The experiment was repeated at least three times and showed comparable results.

Statistical analysis

Pigmentation of engineered strains was categorized as white, pink, red, and dark red. The statistic effect of the type of *PUL* gene (*PUL1* or *PUL2*), *PUL* gene copy numbers (between 0–6), and integration site (chromosome V or VII) on the pigmentation category was tested with a proportional odds model by using the polr function from the MASS R package (Venables and Ripley 2002).

Results

Heterologous expression of *M. pulcherrima* PUL1 and PUL2 confers pulcherrimin production in *S. cerevisiae*

In the past, it has not been possible to produce pulcherriminic acid in *S. cerevisiae* by heterologously expressing genes from *K. lactis* or bacteria and the biochemical activity of *PUL1* is yet unconfirmed (Krause et al. 2018, Widodo and Billerbeck 2022). Here, we have expressed the *M. pulcherrima PUL1* and *PUL2* genes in *S. cerevisiae* and assessed the production of pulcherriminic acid and pulcherrimin by the engineered strains. The ascomycete species *M. pulcherrima* belongs to the CTG clade, while *S. cerevisiae* does not, and thus decodes CTG as serine instead of leucine as in the standard genetic code. For expression in *S. cerevisiae*, the 6 and 8 CTG codons of *PUL1* and *PUL2*, respectively, were therefore changed to AGT codons (encoding serine in *S. cerevisiae*). The sequences were then codon optimized for expression in *S. cerevisiae* using the Twist Bioscience codon optimization tool. Both genes were cloned and integrated in the *URA3* locus, in chromosome V, with the same, strong *TDH3* promoter (P_{TDH3}) and *TDH1* terminator (T_{TDH1}) together with a *LEU2* marker for the selection of transformants (Fig. 1A). This resulted in homologous recombination of the promoter and terminator sequences and the consequential introduction of multiple, random copy numbers of *PUL1* and *PUL2* (Fig. 1B).

Among the transformants growing on the YNB-Leu plates, many white and few colonies with a pinkish or red color were observed. The number of colonies and the frequency of red colonies increased when the amount of DNA used for transformation was increased. Most red transformants grew comparably to the wild-type and stably produced the red phenotype (Fig. 1C). The transformed *S. cerevisiae* strains did not form an apparent red halo around colonies as observed in *M. pulcherrima*, suggesting that pulcherriminic acid is less efficiently secreted in *S. cerevisiae* (Fig. 1C). These results suggested the successful integration of the two *PUL* genes and their function in *S. cerevisiae*.

Confirmation of pulcherriminic acid production by *S. cerevisiae*

Cyclo(Leu–Leu) and pulcherriminic acid are soluble precursors of pulcherrimin, which represents the iron chelate of the latter. In an earlier study, we have proven the presence of pulcherriminic acid in *M. pulcherrima* culture supernatants by sophisticated HPLC HR HESI-MS (Gore-Lloyd et al. 2019). Here, we used the same method to confirm the presence of pulcherriminic acid in the pigmented, engineered strains.

High-resolution mass spectrometry revealed a prominent peak for cyclo(L-leucyl-L-leucyl) (1), and small peaks for pulcherriminic acid (2), as well as the previously identified but uncharacterized intermediates (3), and degradation products (4 and 5) (Fig. 1D) (Gore-Lloyd et al. 2019). A small peak with the same mass as cyclo(L-leucyl-L-leucyl) was observed in the strain lacking *PUL* genes, but none of the intermediates or degradation products could be detected. We thus concluded that the red pigment found in the engineered strains is pulcherriminic acid and that *M. pulcherrima PUL1* and *PUL2* are sufficient to confer pulcherrimin biosynthesis to *S. cerevisiae*.

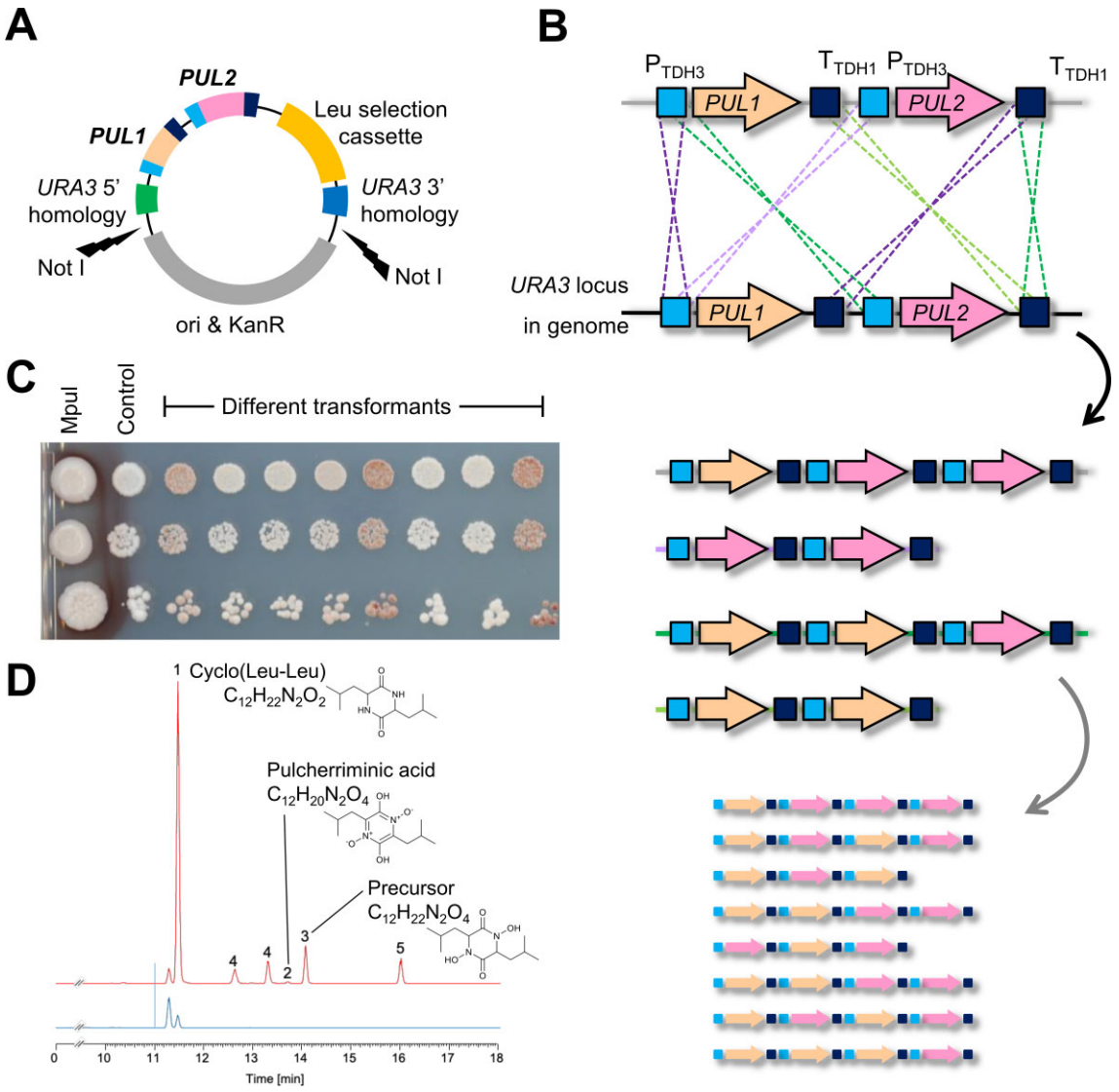

Figure 1. Integration of CTG-corrected and codon optimized *M. pulcherrima* PUL1 and PUL2 genes transfers pulcherrimin formation to *S. cerevisiae*. (A) *PUL1* and *PUL2* were cloned with the *TDH3* promoter (PTDH3) and *TDH1* terminator (TTDH1) and the *LEU2* gene as a selection marker. The construct contained *URA3* 5′ and 3′ homology regions for integration in the *S. cerevisiae* genome. (B) Homologous recombination between the promoter and terminator sequences can lead to the integration of multiple and random numbers of genes. (C) Different transformants grew comparably to the untransformed BY4741 control strain, independent of the color phenotype. The *M. pulcherrima* strain APC 1.2 (Mpul) grew faster and produced a wide, red halo indicative of pulcherrimin formation. (D) Mass spectronomy profile of culture supernatants from a *S. cerevisiae* strain harboring the *M. pulcherrima PUL1* and *PUL2* genes (red trace). All the intermediates and degradation products indicative of pulcherrimin formation were detected. UPLC HR HESI-MS metabolic profiles identified cyclo(Leu–Leu) (1, 227.176 m/z [M + H]+, C12H22N2O2), pulcherriminic acid (2, 257.150 m/z [M + H]+, C12H200N2O4), a precursor (3, 259.165 m/z [M + H]+, C12H22N2O4), and possible degradation products (4 and 5, 275.161 m/z and 229.155 m/z [M + H]+, respectively; C12H22N2O5 and C11H20N2O3, respectively). The *S. cerevisiae* control strain (blue line) only showed a peak with the same retention time as cyclo(Leu–Leu), but none of the other compounds.

PUL1 and PUL2 copy number correlates positively with pulcherrimin production

We have used a systematic metabolic engineering effort by varying the *PUL1* and *PUL2* copy numbers. Homologous recombination with the 5′ and 3′ *URA3* sequences as well as the P_{TDH3} and T_{TDH1} sequences can result in the insertion of random copy numbers of *PUL1* and *PUL2* (Fig. 1B). To infer the number of variable and potentially repetitive insertions that also comprise sequences homologous to wildtype chromosome features, long-read sequencing was used with the expectation that such long reads could traverse relatively large insertions and flanking regions.

In total, we have sequenced 24 different strains that exhibited variation of red coloration, from white to dark red (Fig. 2). As expected, all strains included at least a single copy of *LEU2* and its promoter (strains 387 and 397 contained three copies). In strain 387, three copies of the plasmid vector origin of replication, kanamycin resistance, and its promoter were found. All detected *PUL* genes had upstream *TDH3* promoters. *PUL1* and *PUL2* copy numbers were inferred by BLAST of vector sequences against *de novo* assemblies. Total 17 strains showed agreement in integrated transgene counts between both *de novo* assembly methods, while 7 strains yielded differences between assemblers. QUAST allowed the selection of the best of these assemblies based on metrics for six strains. For strain 411, both draft assemblies were of similarly poor quality. In this case, the Flye assembly was used due to its resolvable transgene integration site (i.e. a single contig). Of

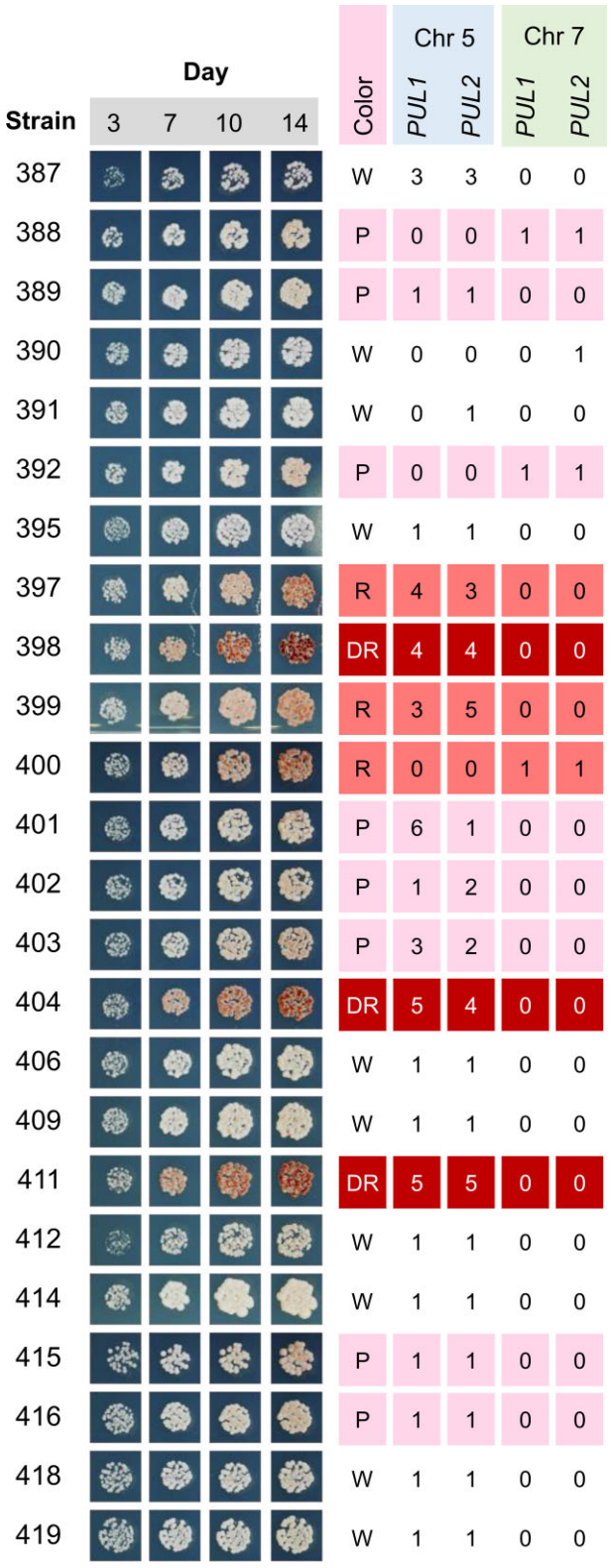

Figure 2. *PUL1* and *PUL2* copy number correlates with pulcherrimin production. The copy numbers and integration sites of the *M. pulcherrima PUL1* and/or *PUL2* genes transferred to *S. cerevisiae* were determined by long-read genome sequencing. Integration was observed at the *URA3* locus on chromosome V, but also in chromosome VII. The red coloration, indicative of pulcherrimin formation, was the strongest in the strains harboring the highest copy number of *PUL1* and *PUL2*. Based on the degree of coloration and the time when coloration was first observed, the strains were categorized as white (W), pink (P), red (R), or dark red (DR).

the 24 strains, 20 had various numbers of *PUL1* and *PUL2* integrations at the *URA3* locus on chromosome V [115 948 (+), breakpoints in alignment to BY4741] (Fig. 2). The maximum number of *PUL1* and *PUL2* genes was 6 and 5, respectively. Total 10 strains contained one copy of each *PUL* gene, which would be expected if there was no recombination between the promoter and terminator sequences. Interestingly, three strains integrated the two genes in chromosome VII, in the *TDH3* promoter (884 491 (–). A fourth strain (390) contained only one copy of the *PUL2* gene in chromosome VII. All strains with integrations in chromosome VII also featured plasmid vector sequences.

To test if the red color depended on the inferred *PUL1* or *PUL2* copy numbers, we assessed the development of the red color, which is indicative of pulcherrimin production, of the 24 transformants qualitatively. In contrast to *M. pulcherrima*, which exhibits its typical red color already after one day on iron-containing culture media, the transformed *S. cerevisiae* strains developed this phenotype over the course of 14 days (Fig. 2). Three strains showed first signs of red coloration after 7 days of growth at 22°C. An additional three strains started to show red coloration at day 10 and for eight strains this was the case at day 14. Over time, the red coloration became stronger and at day 14, we observed three dark red (DR), three red (R), eight pink (P), and 10 white (W) strains. Interestingly, five of the strains harboring one copy of *PUL1* and *PUL2* each (three in chromosome V, two in chromosome VII) were pink, while the remaining seven strains were white. The strain 400, with one copy of each gene integrated in chromosome VII, showed a red phenotype. One strain (387) contained four and two *PUL1* and *PUL2* copies, respectively, but was white. However, this strain seemed to grow slower than the other strains and had multiple vector sequence integrations (see above).

Overall, a clear difference in coloration between strains was apparent and the strains with the strongest pigmentation were those with the highest numbers of integrated *PUL* genes (e.g. strains 411, 404, and 398), while all except one strain categorized as white (387) harbored only one or no copy of a *PUL* gene. These results indicated that integration of more *PUL* genes resulted in a more pigmented phenotype. This was confirmed statistically by testing the effect of the *PUL* gene copy numbers and integration sites with a proportional odds model, where an additional copy of any one *PUL* gene increased the odds of a redder phenotype 1.6-fold (*P*-value = 0.006). Additionally, neither the location (chromosome V or VII) nor the type of *PUL* gene (*PUL1* or *PUL2*) had a significant effect on the odds with *P*-values of 0.386 and 0.781, respectively.

In summary, these results suggest that pulcherrimin production in the *S. cerevisiae* strains correlated positively with the number of the *PUL1* and *PUL2* genes that were integrated in the genome, but was much slower than in *M. pulcherrima*.

Saccharomyces cerevisiae strains with high-level pulcherrimin production reduce conidiation in *Botrytis*

The *S. cerevisiae* strains expressing the *M. pulcherrima PUL* genes produced pulcherrimin only slowly. Filamentous, plant pathogenic fungi grew much faster than the transformed *S. cerevisiae* strains could produce their red phenotype. Conventional competition assays where both fungi are confronted with each other at the same time and growth is quantified are therefore difficult with these pulcherrimin-producing strains. In our preliminary assays, we have seen that *Botrytis* responded to the *S. cerevisiae* strains tested here by producing more or less aerial mycelium and conidia, while radial growth was not affected. We

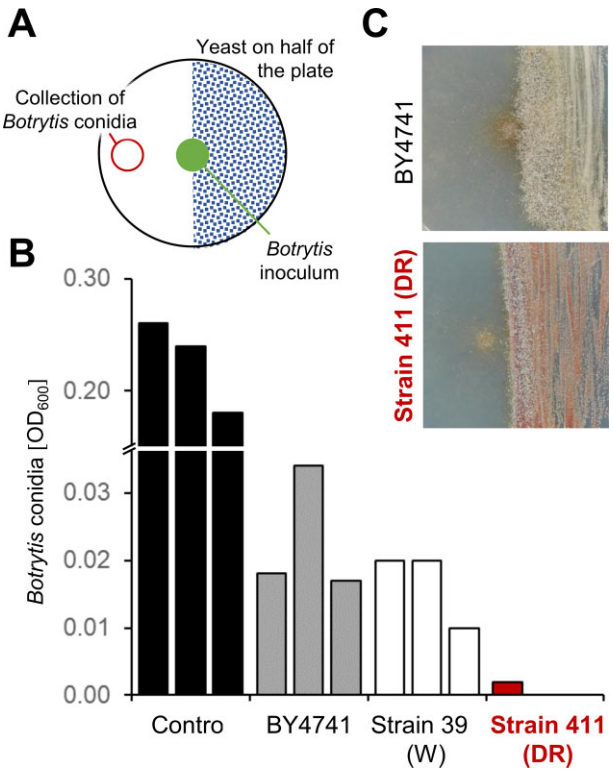

Figure 3. *Saccharomyces cerevisiae* strains with high-level pulcherrimin production inhibit *Botrytis* conidiation. (A) *Saccharomyces cerevisiae* was spread on one half of an agar plate, grown for 1 week, and *Botrytis* was inoculated in the center of the plate. (B) After 10–14 days of co-culture, an agar plug was collected on the side of the plate that was not inoculated with the yeast and *Botrytis* conidia were determined by measuring the OD_{600}. As a control, *Botrytis* was inculated on a plate without yeasts and condia were quantified. (C) Photographs depicting the plates that were used to quantify *Botrytis* conidiation in the presence of different *S. cerevisiae* strains. In most cases, conidia were predominantly formed along the edge of the area colonized by the yeasts.

have therefore developed an assay where we spread the different *S. cerevisiae* strains on one half of an agar plate, let the yeast grow for 1 week, and then inoculate with *Botrytis* in the center of the plate (Fig. 3A). Instead of assessing the growth area in the agar, we then quantified *Botrytis* conidia that were produced on the plates containing the different yeasts (but in the part of the plate that was devoid of yeasts).

The results from these experiments show that a strain with a more pigmented phenotype (e.g. strain 411) strongly reduced the number of conidia produced by *Botrytis* as compared to strains with no *PUL* gene or with only one copy of each gene (e.g. strains BY4741 or 391, respectively) (Fig. 3B and C). Interestingly, the white, engineered *S. cerevisiae* strain 391 caused increased *Botrytis* conidiation as compared to the BY4741 wildtype, albeit the variability was high. We have also performed experiments with apples that were infected by *Botrytis* and treated with the engineered *Saccharomyces* strains. These experiments showed results comparable to the *in vitro* conidiogenesis assays, but the variability from experiment to experiment was considerable and the differences among the different strains were smaller (Supplementary Fig. S1).

Overall, these competition experiments with engineered *S. cerevisiae* strains and *Botrytis* demonstrate an antifungal activity of pulcherrimin production.

Discussion

Pulcherrimin biosynthesis has been described in different yeast species (e.g. *K. lactis*, *Kluvermyces aestuarii*, *Metschnikowia andauensis*, *Metschnikowia fructicola*, *M. pulcherrima*, and *Zygotorulaspora mrakii*) and also in some bacteria such as *Bacillus subtilis* and *Bacillus licheniformis* (Krause et al. 2018, Arnaouteli et al. 2019, Wang et al. 2020, Horváth et al. 2021). Interestingly, the bacterial and yeast pulcherrimin biosynthesis genes are different and not homologous to each other (Krause et al. 2018). In the past, it has not been possible to transfer pulcherrimin biosynthesis to *S. cerevisiae* by using genes from *K. lactis* or bacteria. Here, we report the generation of pulcherrimin synthesizing *S. cerevisiae* strains that harbor multiple copies of the *M. pulcherrima PUL1* and *PUL2* genes. We have confirmed pulcherrimin production in the engineered strains by mass spectrometric identification of pulcherrimin precursors and degradation products and show that the engineered strains inhibited conidiation of the plant pathogen *B. caroliana*.

In some strains only harboring one copy of each *PUL* gene, we have observed a slightly pink phenotype indicative of pulcherrimin formation. At the moment, it is not clear why this phenotypic variation was observed in strains that were determined to harbor the same number of *PUL1* and *PUL2* genes in the same locus. However, strong pulcherrimin formation within 14 days required multiple copies of each gene and the pigmentation correlated positively with the *PUL1* and *PUL2* copy number. It is also not clear why pulcherrimin formation could not be engineered with bacterial or yeasts genes in the past, but since *M. pulcherrima* is a particularly strong pulcherrimin producer, its Pul1 and Pul2 enzymes may be more active. Nevertheless, transformed *S. cerevisiae* strains formed pulcherrimin much slower than *Metschnikowia* does and neither seemed to secrete the molecule in significant amounts, as no red halo was observed around the yeast colonies. At the moment, it is not clear why pulcherrimin formation is thus much less efficient in *S. cerevisiae* as compared to *M. pulcherrima*. In *B. licheniformis*, extensive metabolic engineering (e.g. promoter changes, increased leucine supply, overexpressed leucine-tRNA, and exporter genes) was used to improve pulcherrimin formation with the bacterial genes (Wang et al. 2020, Yuan et al. 2020). It is likely that similar engineering steps will be necessary to improve pulcherrimin production in *S. cerevisiae* and with the *Metschnikowia* genes. It is also noteworthy that our assays were performed at 22°C (competition assays are performed at this temperature and *M. pulcherrima* also grows better at lower temperatures), which is not an optimal growth temperature for *S. cerevisiae*. The results also document that the four *PUL* genes are not sufficient for effective pulcherrimin formation or that the proteins encoded by the *PUL3* and *PUL4* genes, which are still present in the *S. cerevisiae* genome, have lost their original functions. The strains generated here are an ideal tool for further elucidating the pulcherrimin biosynthesis pathway and identifying the missing components required for strong pulcherrimin formation in *S. cerevisiae*. The power of *S. cerevisiae* as a model organism will not only allow optimizing pulcherrimin production, but also facilitate identifying how this molecule is synthesized, secreted, taken up, and metabolized.

In 21 of the 24 *S. cerevisiae* strains studied and described here, the *PUL* genes were integrated at the targeted *URA3* locus. In three strains, integration also occurred in chromosome VII, in the *TDH3* promoter. In chromosome VII, only one copy of each gene or a single *PUL2* gene was detected. In nine strains, multiple copies of both genes (between two and six) were integrated in chromosome V. In the course of our work, we have thus integrated random

copy numbers of *PUL1* and *PUL2* into the *S. cerevisiae* genome due to homologous recombination between the identical promoter and terminator sequences used for *PUL1* and *PUL2* expression. The integration in chromosome VII can be explained by homologous recombination with the *TDH3* promoter. Transfer of heterologous genes with identical promoter and terminator sequences, as we have done in this study, might be an efficient method that could be applied to process-engineering projects that require gene dosage optimization. In particular, when selecting for a visible phenotype such as pulcherrimin formation, the creation of random copy numbers and combinations of two or more genes, including strains with unequal copy numbers of the two genes, can be advantageous. It is possible that one gene is the limiting factor for a biosynthetic process and that uneven copy numbers of two genes are thus selected. In the case of pulcherrimin formation, this was not the case and the strongest producers had equal or similar *PUL1* and *PUL2* copy numbers.

The *S. cerevisiae* strain with the highest number of *PUL1* and *PUL2* integrations (411) exhibited red coloration already after 7 days and inhibited conidiogenesis of the plant pathogenic fungus *Botrytis* more strongly than a control strain. This result was obtained despite the slow production of pulcherrimin and the lack of pulcherriminic acid secretion into the agar. Further optimizing the pulcherrimin biosynthesis pathway in *S. cerevisiae* and engineering pulcherriminic acid secretion would thus likely further improve the observed antagonistic activity. The results presented here confirm that pulcherrimin formation constitutes an effective and promising biocontrol mechanism.

Author contributions

M.M.: conceptualization, cloning, transformation, and data analysis; M.Mc.C.: genome sequencing, data analysis, and writing; A.O.B.: mass spectrometry; L.N.: methodology and data analyzation, L.M.: cloning; S.H.: genome sequencing, data analysis, and writing; M.H.-B.: competition assays and transformation; J.P.: mass spectrometry and supervision; Y.C.: genome analyses, supervision, and writing; F.M.F.: administration, conceptualization, supervision, and writing.

Acknowledgments

We highly appreciate the contributions from Marco Monti and Laurin Müller, who performed initial experiments and analyses at the beginning of the project. We thank Christian Ahrens and Markus Künzler for helpful discussions during the course of this project.

Supplementary data

Supplementary data are available at *FEMSYR* online.

Conflict of interest: The authors declare that they have no competing interests.

Funding

F.M.F. is supported by the Swiss National Science Foundation (SNSF) grant 31003A_175665. This work is also supported by UK Biotechnology and Biological Sciences Research Council (BBSRC) grants BB/M005690/1, BB/P02114X/1, and BB/W014483/1, Engineering and Physical Sciences Research Council (EPSRC) EP/V05967X/1, and a Volkswagen Foundation the "Life? Initiative" Grant (Ref. 94 771) to Y.C.

References

Alonge M, Lebeigle L, Kirsche M *et al.* Automated assembly scaffolding using RagTag elevates a new tomato system for high-throughput genome editing. *Genome Biol* 2022;**23**:258.

Angelini LL, Dos Santos RAC, Fox G *et al.* Pulcherrimin protects *Bacillus subtilis* against oxidative stress during biofilm development. *NPJ Biofilms Microbiomes* 2023;**9**:50.

Arnaouteli S, Matoz-Fernandez DA, Porter M *et al.* Pulcherrimin formation controls growth arrest of the *Bacillus subtilis* biofilm. *Proc Natl Acad Sci USA* 2019;**116**:13553–62.

Bellezza I, Peirce MJ, Minelli A. Cyclic dipeptides: from bugs to brain. *Trends Mol Med* 2014;**20**:551–8.

Bonnefond L, Arai T, Sakaguchi Y *et al.* Structural basis for nonribosomal peptide synthesis by an aminoacyl-tRNA synthetase paralog. *Proc Natl Acad Sci USA* 2011;**108**:3912–7.

Borthwick AD. 2,5-Diketopiperazines: synthesis, reactions, medicinal chemistry, and bioactive natural products. *Chem Rev* 2012;**112**:3641–716.

Bühlmann A, Kammerecker S, Müller L *et al.* Stability of dry and liquid *Metschnikowia pulcherrima* formulations for biocontrol applications against apple postharvest diseases. *Horticulturae* 2021;**7**:459.

Canale-Parola E. A red pigment produced by aerobic sporeforming bacteria. *Archiv Mikrobiol* 1963;**46**:414–27.

Charron-Lamoureux V, Haroune L, Pomerleau M *et al.* Pulcherrimin: a bacterial swiss army knife in the iron war. 2022, DOI: 10.21203/rs.3.rs-2023345/v1.

Coster WD. Chopper. 2023.

Cryle MJ, Bell SG, Schlichting I. Structural and biochemical characterization of the cytochrome P450 CypX (CYP134A1) from *Bacillus subtilis*: a cyclo-L-leucyl-L-leucyl dipeptide oxidase. *Biochemistry* 2010;**49**:7282–96.

De Coster W, D'Hert S, Schultz DT *et al.* NanoPack: visualizing and processing long-read sequencing data. *Bioinformatics* 2018;**34**:2666–9.

Duplex Tools. Oxford Nanopore Technologies. 2023. https://github.com/nanoporetech/duplex-tools

Freimoser FM, Rueda-Mejia MP, Tilocca B *et al.* Biocontrol yeasts: mechanisms and applications. *World J Microbiol Biotechnol* 2019;**35**:154.

Furukawa T, Akutagawa T, Funatani H *et al.* Cyclic dipeptides exhibit potency for scavenging radicals. *Bioorg Med Chem* 2012;**20**:2002–9.

Gondry M, Sauguet L, Belin P *et al.* Cyclodipeptide synthases are a family of tRNA-dependent peptide bond-forming enzymes. *Nat Chem Biol* 2009;**5**:414–20.

Gore-Lloyd D, Sumann I, Brachmann AO *et al.* Snf2 controls pulcherriminic acid biosynthesis and antifungal activity of the biocontrol yeast *Metschnikowia pulcherrima*. *Mol Microbiol* 2019;**112**:317–32.

Gurevich A, Saveliev V, Vyahhi N *et al.* QUAST: quality assessment tool for genome assemblies. *Bioinformatics* 2013;**29**:1072–5.

Hilber-Bodmer M, Schmid M, Ahrens CH *et al.* Competition assays and physiological experiments of soil and phyllosphere yeasts identify *Candida subhashii* as a novel antagonist of filamentous fungi. *BMC Microbiol* 2017;**17**:4.

Horváth E, Dályai L, Szabó E *et al.* The antagonistic *Metschnikowia andauensis* produces extracellular enzymes and pulcherrimin, whose production can be promoted by the culture factors. *Sci Rep* 2021;**11**:10593.

Kántor A, Hutková J, Petrová J *et al.* Antimicrobial activity of pulcherrimin pigment produced by *Metschnikowia pulcherrima* against various yeast species. *J Microb Biotech Food Sci* 2015;**5**:282–5.

Kluyver AJ, Vanderwalt JP, Vantriet AJ. Pulcherrimin, the pigment of *Candida pulcherrima*. *Proc Natl Acad Sci USA* 1953;**39**:583–93.

Kolmogorov M, Yuan J, Lin Y *et al.* Assembly of long, error-prone reads using repeat graphs. *Nat Biotechnol* 2019;**37**:540–6.

Koren S, Walenz BP, Berlin K *et al.* Canu: scalable and accurate long-read assembly via adaptive k-mer weighting and repeat separation. *Genome Res* 2017;**27**:722–36.

Krause DJ, Kominek J, Opulente DA *et al.* Functional and evolutionary characterization of a secondary metabolite gene cluster in budding yeasts. *Proc Natl Acad Sci USA* 2018;**115**:11030–5.

Lee ME, DeLoache WC, Cervantes B *et al.* A highly characterized yeast toolkit for modular, multipart assembly. *ACS Synth Biol* 2015;**4**:975–86.

Li H. Minimap2: pairwise alignment for nucleotide sequences. *Bioinformatics* 2018;**34**:3094–100.

Li H. New strategies to improve minimap2 alignment accuracy. *Bioinformatics* 2021;**37**:4572–4.

Li H, Handsaker B, Wysoker A *et al.* The sequence alignment/map format and SAMtools. *Bioinformatics* 2009;**25**:2078–9.

MacDonald JC. Biosynthesis of pulcherriminic acid. *Biochem J* 1965;**96**:533–8.

Melvydas V, Staneviciene R, Balynaite A *et al.* Formation of self-organized periodic patterns around yeasts secreting a precursor of a red pigment. *Microbiol Res* 2016;**193**:87–93.

Mishra AK, Choi J, Choi S-J *et al.* Cyclodipeptides: an overview of their biosynthesis and biological activity. *Molecules* 2017;**22**:1796.

Randazzo P, Aubert-Frambourg A, Guillot A *et al.* The MarR-like protein PchR (YvmB) regulates expression of genes involved in pulcherriminic acid biosynthesis and in the initiation of sporulation in *Bacillus subtilis*. *BMC Microbiol* 2016;**16**:190.

Saravanakumar D, Clavorella A, Spadaro D *et al.* *Metschnikowia pulcherrima* strain MACH1 outcompetes *botrytis cinerea*, *alternaria alternata* and *penicillium expansum* in apples through iron depletion. *Postharvest Biol Technol* 2008;**49**:121–8.

Sedlazeck FJ, Rescheneder P, Smolka M *et al.* Accurate detection of complex structural variations using single-molecule sequencing. *Nat Methods* 2018;**15**:461–8.

Sipiczki M. *Metschnikowia* strains isolated from botrytized grapes antagonize fungal and bacterial growth by iron depletion. *Appl Environ Microb* 2006;**72**:6716–24.

Tang MR, Sternberg D, Behr RK *et al.* Use of transcriptional profiling & bioinformatics to solve production problems: eliminating red pigment production in a *Bacillus subtilis* strain producing hyaluronic acid. *Ind Biotechnol* 2006;**2**:66–74.

Venables WN, Ripley BD. *Modern Applied Statistics with S*. New York, NY: Springer, 2002.

Wang D, Zhan Y, Cai D *et al.* Regulation of the synthesis and secretion of the iron chelator cyclodipeptide pulcherriminic acid in *Bacillus lichen i formis*. *Appl Environ Microb* 2018;**84**:e00262–18.

Wang S, Wang H, Zhang D *et al.* Multistep metabolic engineering of *Bacillus licheniformis* to improve pulcherriminic acid production. *Appl Environ Microb* 2020;**86**:e03041–19.

Wick RR, Schultz MB, Zobel J *et al.* Bandage: interactive visualization of *de novo* genome assemblies. *Bioinformatics* 2015;**31**:3350–2.

Widodo WS, Billerbeck S. Natural and engineered cyclodipeptides: biosynthesis, chemical diversity, and engineering strategies for diversification and high-yield bioproduction. *Engineer Microbiol* 2022:100067.

Yuan S, Yong X, Zhao T *et al.* Research progress of the biosynthesis of natural bio-antibacterial agent pulcherriminic acid in *Bacillus*. *Molecules* 2020;**25**:5611.

Received 8 August 2023; **accepted** 21 December 2023